Inst. Phys. Conf. Ser. No 153: Section 2
Paper presented at Electron Microscopy and Analysis Group Conf. EMAG97, Cambridge, 1997

Aberration correction in the STEM

OL Krivanek*, N Dellby*, AJ Spence, RA Camps and LM Brown**

MP group, Cavendish Laboratory, University of Cambridge, Cambridge CB3 0HE, UK
* now at: Dept. of Materials Science, Roberts Hall, U. of Washington, Seattle WA 98195, USA
** now at: Dept. of Applied Physics, Cornell University, Ithaca NY 14853, USA

ABSTRACT: A quadrupole-octupole spherical aberration corrector has been designed and built for a modified VG HB5 STEM. The corrector fits between the second condenser and the objective lens, and consists of 6 separate stages. Each stage contains one strong quadrupole, one strong octupole and 12 auxiliary trim coils. The corrector is provided with autotuning software that measures all the relevant aberrations on-line and tunes the corrector automatically. Preliminary tests of the corrector have verified the correction principle, and shown that it can readily compensate for parasitic aberrations arising from misalignment.

1. INTRODUCTION

Aberration correction in electron microscopy is a subject with a 60 year history dating back to the fundamental work of Scherzer (1936, 1947). There have been many partial successes, such as Deltrap's quadrupole-octupole corrector which nulled spherical aberration (C_s) over 30 years ago (Deltrap 1964a, 1964b). More recently, an electromagnetic sextupole-round lens-sextupole corrector built for a conventional transmission electron microscope (CTEM) by Haider et al. (1995), and a mostly-electrostatic quadrupole-octupole corrector of both spherical and chromatic (C_s and C_C) aberration built by Zach and Haider (1995) for a scanning electron microscope (SEM) have both demonstrated an improvement of resolution in their respective microscopes. Nevertheless, the practical goal of attaining better resolution than had ever been reached by any other microscope operating at the same voltage appears to remain unfulfilled.

2. A QUADRUPOLE-OCTUPOLE CORRECTOR FOR A DEDICATED STEM

A scanning transmission electron microscope (STEM) with corrected spherical aberration would produce a smaller probe size at a given beam current than an uncorrected STEM, and a larger beam current in a probe of a given size. C_s correction in STEM is thus expected to provide more tangible benefits than in CTEM, where the optimum C_s value for phase contrast imaging is non-zero and the "information limit" resolution is typically determined by chromatic aberration.

Sextupole-round lens-sextupole correctors cannot be extended to C_C correction, and electrostatic correctors are not suitable for beam energies above around 30 keV. Keeping in mind that C_C will limit the resolution of a C_s-corrected microscope, the corrector we have designed and built for our VG HB5 dedicated STEM is an electromagnetic quadrupole-octupole C_s corrector that is compatible with incorporating C_C correction in the future. The VG HB5 has an objective lens with C_s = 3.5 mm and C_C = 3.5 mm. In the standard microscope operating mode, the lens only demagnifies the probe by 25x and gives a best dark field resolution of about 0.4 nm. The corrector has been built as a proof-of-principle instrument designed to impart negative spherical aberration to the electron beam and thereby compensate the positive spherical aberration of the microscope's other lenses. Improvements in the microscope performance beyond what can be achieved in the best current 100 kV STEMs are expected only when the objective lens is modified to provide smaller starting C_s and C_C, and larger demagnification.

The corrector consists of 6 identical stages, each one of which comprises a strong quadrupole and a strong octupole. The quadrupole windings are distributed on the 12 poles in a way that approximates an ideal quadrupole up to 8th order, and the octupoles are ideal up to 6th order. There is also a separate weak auxiliary winding on each pole. Computer-controlled current supplies with 1 ppm stability are provided for each quadrupole, octupole and auxiliary winding. Software running under Microsoft NT operating system allows any number of the power supplies to be linked together with adjustable strengths and labeled as a new control, i.e. it provides the flexibility needed to compensate for imperfections of the principal quadrupoles and octupoles and also to create weak independent dipoles, quadrupoles, sextupoles and octupoles of arbitrary orientation. The electronics also sends currents to 4 sets of alignment coils and voltages to an 8-pole deflector that was used as an objective lens stigmator in the HB5 and now serves as an objective lens alignment coil, for a total of 96 computer-controlled power supplies. Because of the low power required by quadrupoles and octupoles and the high packing density of our design, the corrector electronics fits into an enclosure of 50x46x28 cm.

The quadrupole excitations are antisymmetric about the mid-plane of the corrector. The first-order trajectories are thus constrained by 3 independent parameters, which allows enough flexibility to couple the corrector to an entrance crossover situated within a range of distances D from the corrector (Fig. 1). The corrector produces a 1:1 magnification, pre-aberrated image of the crossover D away from the exit face of the corrector. The corrector is placed between the second condenser lens and the scan coils preceding the objective lens (Fig. 2). Because the scan coils are placed after the corrector, aberrations depending on the off-axis position in the image plane become unimportant. Varying the distance D of the exit crossover from the corrector allows the beam diameter inside the corrector and the post-corrector demagnification to be varied.

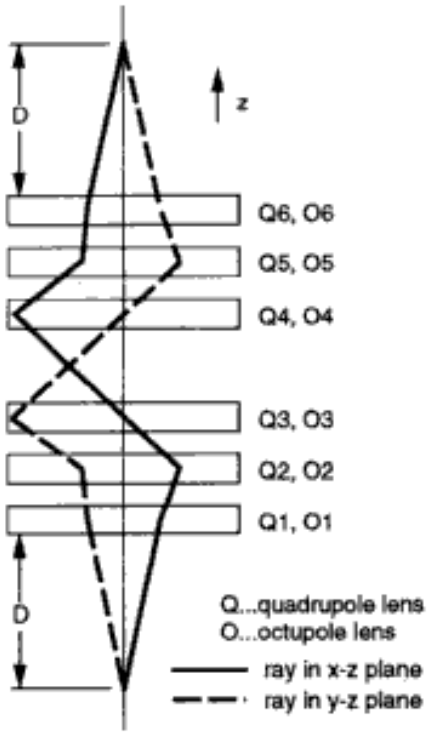

Fig. 1 Schematic diagram of the quadrupole-octupole corrector and of the electron trajectories through it.

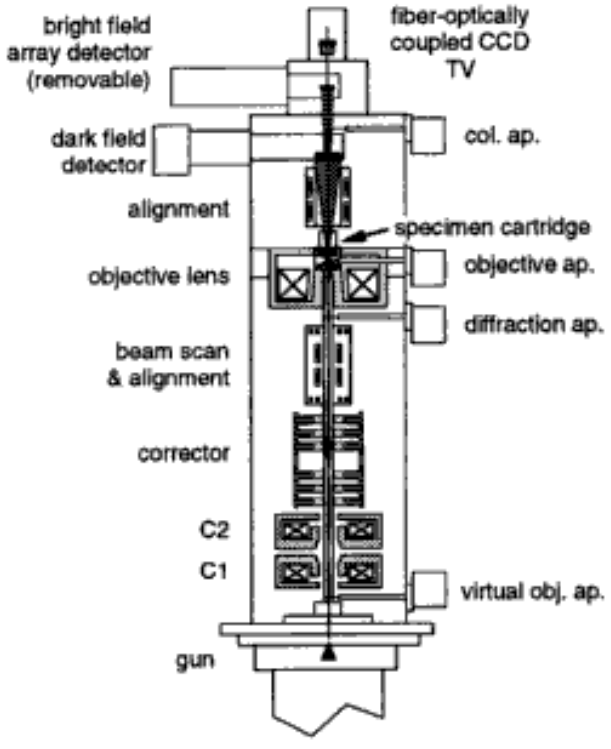

Fig. 2 Placement of the corrector in the modified HB5 column.

Because quadrupoles and octupoles don't have the cylindrical symmetry of round lenses, three principal third order aberrations need to be considered: the normal spherical aberration ($C_{3,0}$=C_s), 2-fold astigmatism of spherical aberration ($C_{3,2}$) and 4-fold astigmatism ($C_{3,4}$). Octupole O3, which contains an x-focus line, acts on all three coefficients, in proportions 1, -4/3, 1/3. O4, which contains a y-focus line, also acts on all three, but in proportions 1, 4/3,

1/3. Exciting O3 and O4 equally thus makes it possible to adjust the spherical aberration coefficient to any desired value, but also results in 4-fold astigmatism. The 4-fold astigmatism can, however, be removed by any octupole in which the beam is round, without affecting the other two aberrations. This is exactly the case in octupoles O1 and O6, and approximately the case in octupoles O2 and O5. We excite these four octupoles approximately equally, as this gives about the same absolute excitation (and hence the same field strength and saturation characteristics) in all the octupoles of the corrector.

Further key components of our system are a fiber-optically coupled TV camera which captures the shadow image appearing in the detector plane, a retractable bright field detector using a YAP scintillator, and a computer-based scanned image acquisition system (Gatan DigiScan plus Power Macintosh) running under DigitalMicrograph image acquisition and processing software. The VG column has been modified by adding a second condenser lens, extra illumination alignment coils and of course the corrector. An overall system diagram is shown in Fig. 3.

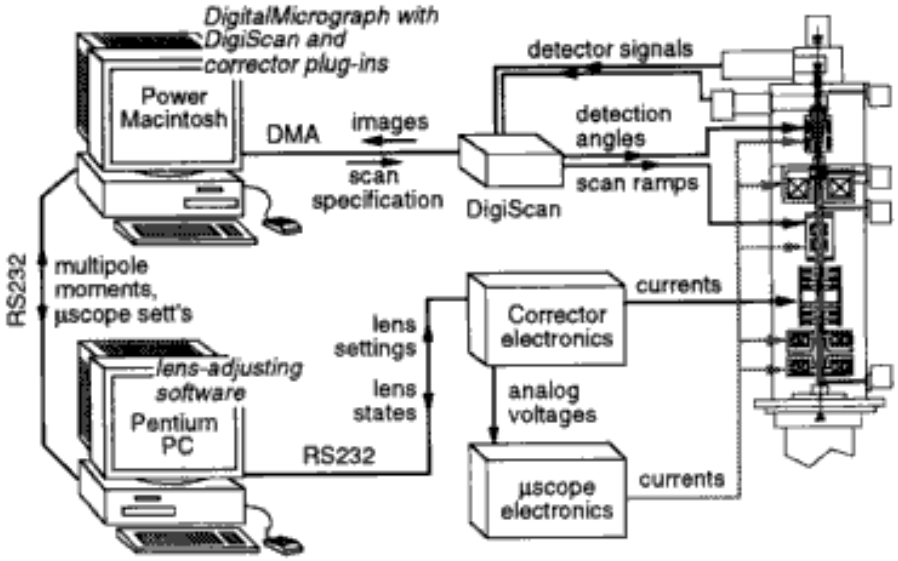

Fig. 3 System diagram of the corrector.

We have also modified the vacuum system of the upper column by replacing the VG diffusion pump, liquid N_2 trap and mechanical rotary pumps by an all-dry pumping system consisting of two ion pumps (270 and 25 l/s) plus a molecular drag pump backed by a diaphragm pump. Vacuum levels about 4x better than previously have been attained, especially in the critical gun valve region of the microscope, which is now pumped by the 25 l/s ion pump separately from the rest of the system.

3. ABERRATION DIAGNOSIS

Trying to correct spherical aberration without having a method for identifying and measuring all the aberrations up to third order can lead to a situation where one is faced with a fuzzy image, a large number (>10) of controls and no useful procedure for making the image sharper. In the STEM, two different methods for diagnosing the aberrations are available: visual examination of far-field shadow images (Ronchigrams), and acquiring images recorded with different detection angles and comparing them in the computer. The second method is related by reciprocity to TEM bright field autotuning using images acquired with different illumination angles (Krivanek and Fan, 1994).

Either method allows one to characterize the aberration function. Recording Ronchigrams requires simply an efficient two-dimensional detector such as our fiber-optically coupled TV. The second method requires software and hardware that can vary the detection angle using the microscope Grigson coils, record a tableau of the required images, analyze either the variation in their absolute position or in their apparent defocus and/or astigmatism, and

microscope, and found the manual Ronchigram method to be especially useful for initial set-up, and the automated image tableau method best suited for fine-tuning and precise measurement of the aberrations. Examples of results of both methods are shown in the next section.

When running the autotuning software on the microscope at probe currents 0.5 nA and greater prior to the incorporation of the corrector, we measured the C_S of the entire microscope as 7 mm and larger (we obtained values as large as 120 mm). This is because in the large current mode the source is demagnified less, and the gun makes an appreciable contribution to the total C_S. A corrected microscope will therefore give dramatically smaller probes at 0.5 nA and larger currents, providing an extra reason for C_S correction in the STEM.

4. PRELIMINARY RESULTS FROM THE CORRECTOR

At the time of writing of this manuscript, the corrector had been operational for a total "beam time" of about 3 weeks. This has proved enough to verify the correction principle we use, but not enough to fully optimize the operation of the corrector.

First tests of the corrector verified that the magnetic fields produced by the principal quadrupoles of the 6 stages are concentric to each other within ±40 μm. This has been achieved without altering the number of turns on each pole to perfect the field shape. It is slightly better than what we expected from tolerance buildup and inhomogeneity of the polepiece material. It is very welcome as it allows us to reduce the strength of the trim coils from 10% to 3% of the excitation of the quadrupoles and the octupoles, and thus to decrease the influence of the trim coils on the stability of the total system.

When deciding on the best first order trajectories through our system, the single most important parameter is the ratio of the beam diameter in the corrector to the beam diameter in the objective lens (OL). Increasing the beam diameter in the corrector by 2x while keeping the diameter in the OL the same increases the corrector's effectiveness by 16x. The diameter ratio is determined by the position of the beam crossover between the corrector and the OL. In our system, locating the crossover at the diffraction aperture (see Fig. 2) would give a corrector capable of correcting C_S of up to about 200 mm, but also result in increased instabilities. We therefore lower the crossover position roughly to the middle of the scan coils, and obtain a system capable of correcting C_S up to about 8 mm with the present objective lens.

Once the crossover position is fixed, the next important choice is the overall demagnification of the "virtual" source (as seen by the first condenser). For high resolution operation we demagnify about 80x, for high current operation about 10x. Together with the requirements that the corrector quadrupoles be antisymmetric and that the entrance and exit crossover distances for the corrector be identical, this determines the required excitations of the two condensers and of the corrector quadrupoles.

Fig. 4 shows a shadow image (Ronchigram) obtained on the fiber-optically coupled TV when the corrector's quadrupoles were on and octupoles off. Positive spherical aberration of the microscope demonstrates itself by the circle of infinite azimuthal magnification (marked) and the circle of infinite radial magnification at 0.58 the radius of the azimuthal circle.

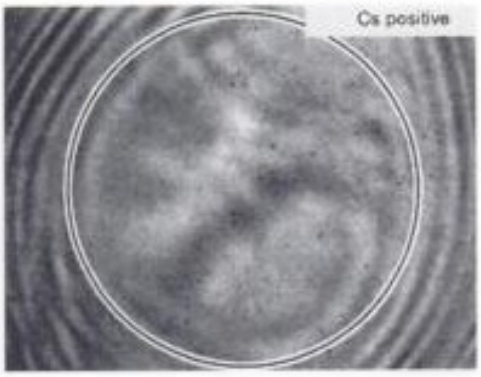

Fig. 4 Underfocus Ronchigram recorded with the corrector's quadrupoles on and octupoles off. Angular range ~ ±10 mrad.

Fig. 5 shows a Ronchigram obtained with both the quadrupoles and the octupoles on. The octupoles were stronger than required for C_S compensation. As a result, the whole system had negative spherical aberration, demonstrated by an overfocused central part of the Ronchigram (revealed by the dark fringe inside the hole image near the center) surrounded by a

circle of infinite radial magnification. (Had C_s been positive, an overfocused central part could not have any infinite magnification circles around it.)

Fig. 6 shows a Ronchigram obtained with the octupole excitation scaled back to the value required for total system $C_s = 0$. Since a perfectly focused and aberration-corrected microscope gives an uninformatively uniform contrast in a Ronchigram, the objective lens was underfocused by about 400 nm. This has produced a Ronchigram that has uniform magnification, as expected for a C_s-corrected STEM free of parasitic aberrations. The microscope had been tuned manually simply by observing Ronchigrams and compensating for successively higher order aberrations using the appropriate controls, starting with first order aberrations (defocus and astigmatism) and finally fine-tuning the 3rd order coefficients (C_s, 2-fold astigmatism of C_s, and 4-fold astigmatism).

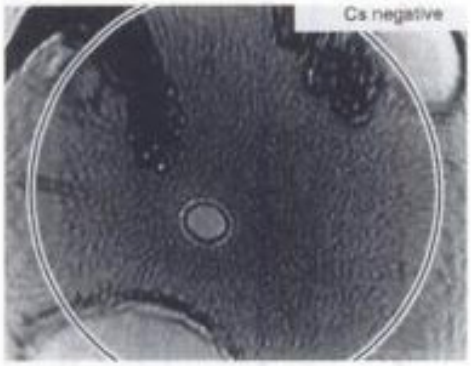

Fig. 5 Ronchigram recorded with the octupoles stronger than needed for C_s correction. Angular range ~ ±10 mrad.

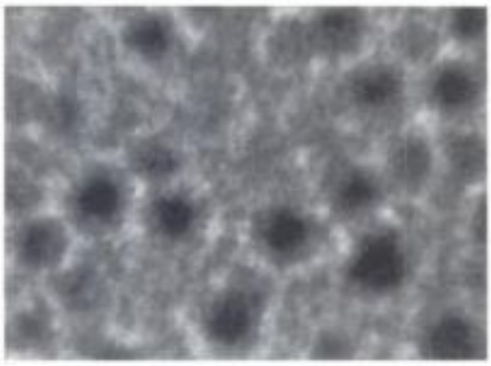

Fig. 6 Ronchigram recorded with the octupoles at the correct excitation. Angular range ~ ±10 mrad.

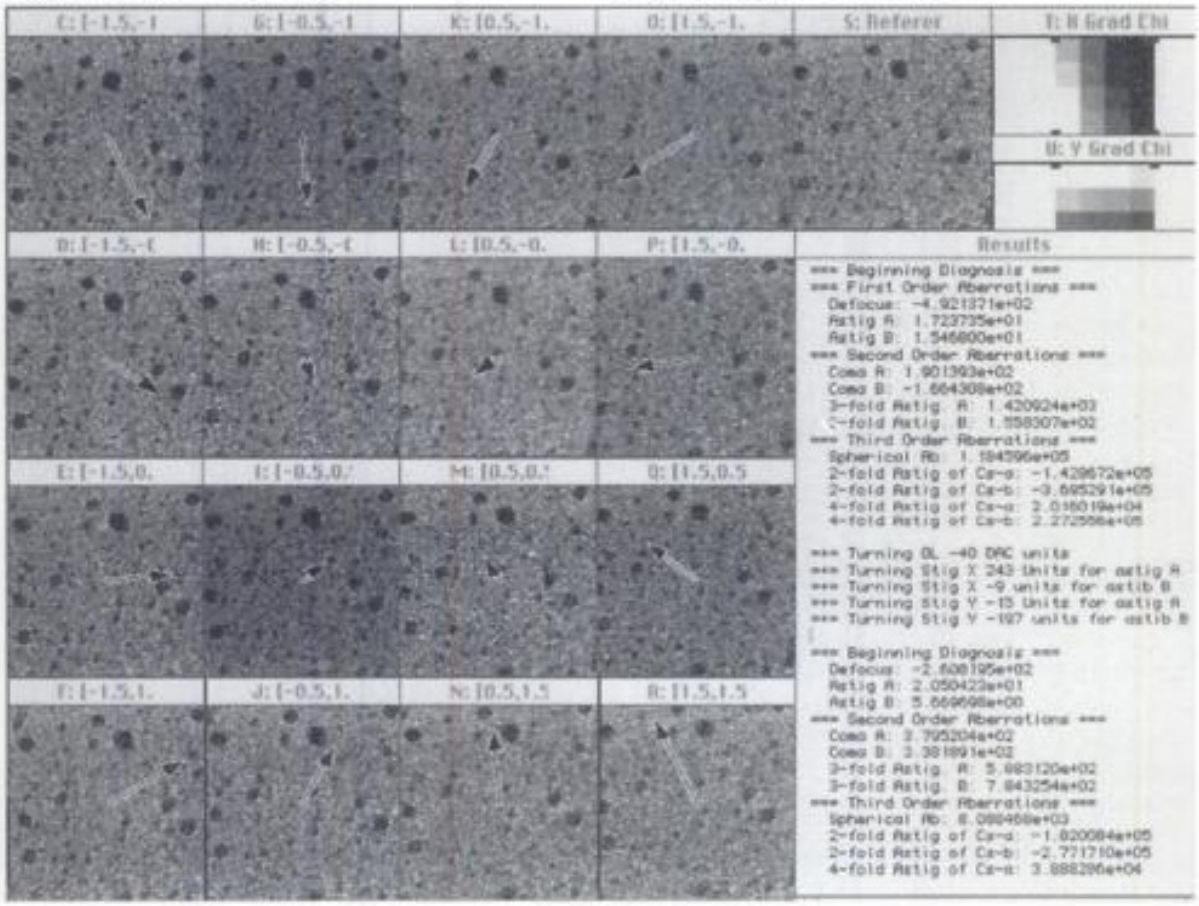

Fig. 7 Automated aberration diagnosis of the corrected microscope.

Fig. 7. shows the results of running the aberration diagnosis software on the microscope shortly after recording the Ronchigram shown in Fig. 6. The gold particles visible in the images are 3-5 nm in diameter. The injected detection tilt increment between neighboring images was 5 mrad. The arrows superimposed on the tableau images show the relative displacement of the images with respect to the reference image (after subtraction of a spurious shift diagnosed by detecting large angle dark field images under identical conditions). The X and Y components of the arrows are grouped together in the "X grad Chi" and "Y grad Chi" images. These are fitted with 2-dimensional third order polynomials, and the polynomial coefficients translated into aberration coefficients. The results for the present tableau are shown in the bottom half of the Results window, with all the aberrations in nm. The top half shows the results of the preceding diagnosis run with the same microscope set-up (to show the repeatability of the analysis). The results can be summarized as follows:

2nd order aberrations (coma a, b; 3-fold astigmatism a, b): all less than 1 μm
C_S: less than 0.12 mm
other third order aberrations: a-type: less than 0.1 mm; b-type: less than 0.4 mm

We made no attempt to correct the b-type third order aberrations, which should be zero in a system with perfect alignment, machining and material homogeneity. The fact that they are less than 10% of the initial C_S again confirms the good mechanical precision that was achieved. With the b-type correction activated and the beam instability (see next paragraph) removed, we expect to be able to keep all 3rd order aberration coefficients easily below 0.1 mm.

Scanned images acquired so far have shown a resolution of about 3 Å in one direction and 5 Å in the perpendicular direction. The resolution loss is due to an instability that is also present with the corrector switched off and disconnected from its power supplies. We are now tracing the origin of this instability, and expect to have improved resolution images shortly.

5. CONCLUSION

The preliminary results described here show that thanks to the excellent flexibility and precision made possible by computer-controlled power supplies and to new methods of on-line aberration diagnosis, C_S correction in our STEM has been achieved. Its benefits in terms of improved resolution and greater current into a given-size probe promise to be considerable.

Perhaps the most exciting aspect of this development is that it is open-ended, with C_C and even C_5 correction using similar principles and techniques presenting themselves as the natural next (though harder) steps. The road should ultimately lead to an era of lab-sized STEM instruments able to routinely achieve 1 Å or even 0.5 Å resolution, and to deliver probe currents into atom-sized sample regions that are large enough for rapid and sensitive EELS and EDXS microanalysis. Such instruments will be able to image and determine the chemical types of individual atoms in many kinds of materials, and thereby bring benefits to the Materials Science community that are just as revolutionary as those brought to astronomy by the *aberration-corrected* Hubble space telescope.

6. ACKNOWLEDGMENT

We are grateful to the Paul Instrument Fund for financial support, the Cavendish Laboratory for provision of facilities, Gatan R&D for surplus equipment and Drs. S. von Harrach and A. Waye for advice on VG matters.

REFERENCES

Deltrap JHM 1964a Ph.D. thesis, U. of Cambridge
Deltrap JHM 1964b Proc 3rd EUREM Congress (Prague) 45
Haider M, Braunshausen G and Schwan E 1995 Optik **99**, 167
Krivanek OL and Fan GY 1994 Scanning Microscopy Supplement **6**, 105
Scherzer O 1936 Zeitschrift Physik **101**, 593
Scherzer O 1947 Optik **2**, 114
Zach J and Haider M 1995 Optik **99**, 112